Role of Global Longitude Strain related miRNAs as potential prognostic indicators in myocardial infarction

Xiaozhu Chen (xzchen66@yeah.net)
People's hospital of Longhua District
Fengrong Huang
People's hospital of Longhua District
Yunhong Liu
People's hospital of Longhua District
Shujun Liu
People's hospital of Longhua District
Gangwen Tan
People's hospital of Longhua District

Research Article

Keywords: surgical therapy, myocardial infarction, real-time three-dimensional spot tracking echocardiography (RT3D-STE), differential expression microRNAs, exosomes.

Posted Date: January 18th, 2022

DOI: https://doi.org/10.21203/rs.3.rs-1227332/v1

Abstract

BACKGROUND

Real-time three-dimensional spot tracking echocardiography (RT3D-STE) can be used to assess the prognosis of myocardial infarction (MI). Analyzing the correlation between miRNAs and RT3D-STE, especially miRNAs and Global Longitude Strain (GLS) and Global Circumferential Strain (GCS), can provide new ideas for discovering and evaluating the role of miRNAs in assessing myocardial function and prognosis of MI.

METHODS

The present study collected forty-nine (49) plasma samples (15 normal samples and 34 MI samples; 22 before and 12 after intervention therapy) and employed high-throughput sequencing technology and real-time quantitative polymerase chain reaction (qRT–PCR) to identify the differentially expressed miRNAs. The Pearson correlation coefficient was used to measure the strength of a linear association between differentially expressed miRNAs and strain parameters of RT3D-STE.

RESULTS

One hundred forty-one (141) differentially expressed plasma exosome miRNAs were identified in STEMI compared with NSTEMI. The target genes of these ten miRNAs were analyzed for Gene Ontology (GO) and Kyoto Encyclopedia of Genes and Genomes (KEGG) pathway enrichment, and they were found to be involved mainly in cellular metabolism processes, HIF-1 signaling pathway, and the FoxO signaling pathway. Moreover, three of these differentially expressed miRNAs (hsa-miR-4798-3p, hsa-miR-371a-3p and hsa-miR-4735-5p) had Pearson correlations greater than 0.5 based on GLS.

CONCLUSION

Differentially expressed miRNAs obtained before and after surgical therapy of MI may play important roles in the occurrence and development of MI. hsa-miR-4798-3p, hsa-miR-371a-3p, and hsa-miR-4735-5p may be used as potential prognostic indicators of MI.

Core Tip

This study aimed to provide relevant evidence for the clinical evaluation of prognosis by exploring differentially expressed miRNAs before and after intervention therapy for MI and their correlation with the strain parameters of RT3D-STE. We identified differentially expressed miRNAs before and after surgical therapy of MI, and their target genes were related to the FoxO signaling pathway and Hippo signaling pathway. These miRNAs may play an important role in the occurrence and development of MI. Some of

these miRNAs (i.e., hsa-miR-4798-3p, hsa-miR-371a-3p, and hsa-miR-4735-5p) are strongly correlated with GLS and may be used as potential prognostic indicators of MI.

1. Introduction

Myocardial infarction (MI) is a common cardiovascular disease that causes irreversible damage to the myocardium due to hypoxia[23], [4,16].It has been shown that MI is one of the most common causes of morbidity and death in the world, and more than one-third of deaths in developed countries are caused by MI each year[12,32]. At present, the main clinical therapy for coronary heart disease is thrombolysis and surgical therapy[22]. However, due to the complexity of the disease and the presence of complications, the prognosis of MI is poor[11]. Therefore, we explored whether there is a specific biomarker that can help in the diagnosis, treatment and prognosis prediction of coronary heart disease.

Exosomes are lipid bilayer vesicles with a diameter of 30-150 nm secreted by cells, containing large number of proteins, nucleic acids, lipids and other bioactive substances, which are key components of intercellular communication[7]. Increasing evidence has indicated that cardiac exosomes affect myocardial hypertrophy, injury and infarction, ventricular remodeling, angiogenesis, and atherosclerosis[6]. MicroRNAs (miRNAs) are single-stranded RNA molecules that measure approximately 21-23 nucleotides in length that are specifically expressed in many tissues, including cardiomyocytes, and are closely related to the occurrence and development of cardiovascular diseases such as myocardial infarction, heart failure, and arrhythmia [15,19,30]. Guo et al. [5] examined the plasma exosomal miRNA profiles of 118 subjects and identified 18 specific miRNAs that may act as potential biomarkers for early MI detection. A recent meta-analysis suggested that circulating miR-1, miR-133, miR-208, and miR-499 showed diagnostic value, while miR-208 showed prognostic predictive value for MI[12]. These studies show that exosomal mRNAs can be used as a potential diagnostic marker for MI. However, there are still few reports on miRNAs differential expression before and after surgical therapy of MI and their roles in assessing cardiac function and prognosis.

Real-time three-dimensional spot tracking echocardiography (RT3D-STE) can track myocardial spot movement in three-dimensional space, and synchronously measure the Global Longitude Strain (GLS), Global Radial Strain (GRS), Global Circumferential Strain (GCS) and Global Area Strain (GAS) of the left ventricle to more sensitively show the strain changes of the ischaemic myocardium, which can be used to assess subtle myocardial damage and assess myocardial viability[1,17]. 3D-STE can be used to assess left atrium (LA) function, and has better repeatability and less load dependence than traditional methods[34]. GLS is now accepted as a marker for subclinical LV dysfunction beyond LVEF in various clinical situations[35]. Recent studies have shown that GLS was the strongest predictor for major adverse cardiac events, and its combination with 3D-GCS could predict them more accurately[9]. Therefore, analyzing the correlation between miRNA and RT3D-STE, especially miRNA and GLS, GCS, can provide new insights for discovering and evaluating the role of miRNA in evaluating the myocardial function and prognosis of MI.

This study is aimed to provide relevant evidence for the clinical evaluation of prognosis by exploring the differentially expressed miRNAs before and after intervention therapy for MI and their correlation with strain parameters of RT3D-STE.

2. Materials And Methods

2.1 Sample collection

The present study was approved by the Research Ethics Committee of Shenzhen Longhua People's Hospital (NO. KY20200801). All ethics procedures conformed with the principles of the 1964 Declaration of Helsinki and its latest 2008 amendment. The research was conducted with the informed consent of each participant, and all participants have signed the informed consent forms. Forty-nine samples (15 normal samples (NC) and 34 MI samples, 22 before (MI) and 12 after surgical therapy (MIAO)) were collected from Shenzhen Longhua People's Hospital. The surgical therapy is Percutaneous Coronary Intervention (PCA), including Percutaneous Transluminal Coronary Angioplasty (PTCA) and Stent implantation.

2.2 Exosome isolation and detection

The clinical specimens were thawed on ice. Then, exosomes were isolated from the plasma using exoQuick precipitation (System Biosciences, USA) according to the manufacturer’s protocol. The extracted exosomes were identified by transmission electron microscope, nanoparticle tracking analysis (NTA, Particle Metrix, Germany) and Western blotting.

2.3 RNA isolation

Total RNA, including miRNA, was extracted using RNA Isolation Reagent (Vazyme, Nanjing, China), according to the manufacturer’s instructions. Additionally, after isopropyl alcohol was added, 1 μg of glycogen was added to each sample. The RNA concentration was measured, and RNA was stored at -80°C for later use. The concentration of RNA was quantified on a NanoDrop 2000 (Thermo, USA) at an absorbance of 260 nm. RNA integrity was determined by agarose gel electrophoresis and with a Bioanalyser 2100 (Agilent Technologies, Santa Clara, CA).

2.4 miRNA sequencing and differential expression analysis

The miRNA library was constructed using the QIAseq miRNA Library Kit (QIAGEN, Germany). The library after quality control was sequenced on an Illumina HiSeq 2500 with the SE50 strategy. The transcripts per million reads (TPM) were calculated to normalize for the RNA depth of sequencing. miRNAs with read counts greater than or equal to 10 were considered to be expressed, while read counts of less than 10 were considered to indicate no expression. miRNAs were defined as differentially expressed when |logFC| was >1 and the FDR (false discovery rate) was <0.01. MiRNAs with logFC >1 were considered to be upregulated, while miRNAs with logFC <−1 were considered to be downregulated.

2.5 Prediction of Gene Ontology (GO) terms and pathways by miRNA targeted genes

Genes targeted by differentially expressed miRNAs were predicted with the use of a public miRTarBase database, and categorized according to their Gene Ontology (GO) terms, which can provide comprehensive information on gene function using topGO (version 2.18.0) software with Fisher's exact test. Pathway identification was performed with KOBAS 2.0 software and hypergeometric tests via the Kyoto Encyclopedia of Genes and Genomes (KEGG) database.

2.6 Real-time Quantitative Polymerase Chain Reaction

To verify our results, the screened miRNAs were analysed by real-time quantitative polymerase chain reaction (qRT–PCR). Total RNA was extracted by the TRIpure Total RNA Extraction Reagent method (ELK Biotechnology, China). RNA concentration and purity were determined by a NanoDrop 2000 (Thermo Fisher Scientific). Takara 638314 (Takara, Japan) was used to synthesize cDNA in one step. PCR amplifications were performed using a StepOnePlus System (Thermo Fisher Scientific). The internal reference gene is U6. The primer sequences used for the evaluated genes are listed in **Supporting** Table 1.

Table 1
Differentially expressed miRNAs between AMI patients compared with normal samples and after AMI compared with preoperatively and their correlation with strain parameters of RT3D-STE

miRNAs	MI-vs-NC	MIAO-vs-MI	strain parameters of RT3D-STE	pearson	p
hsa-miR-4778-3p	down	down	GLS	0.71	0.001
hsa-miR-4798-3p	down	up	GLS	-0.55	0.022
hsa-miR-376c-3p	down	down	GCS	0.51	0.037
hsa-miR-371a-3p	down	up	GLS	-0.54	0.026
hsa-miR-4735-5p	up	down	GLS	-0.59	0.013

2.7 Statistics

Cycle threshold (Ct) values were processed by LightCycler 480 v1.5.0.39 Software. The expression value of miRNAs relative to internal controls was calculated using the $2^{-\triangle\triangle Ct}$ method. Statistical analysis was performed with SPSS software. Data were tested for significance with the nonparametric Mann-Whitney U test. A P value < 0.05 was considered to be significant. Pearson correlation analysis was performed by SPSS 22.0.

3. Results

3.1 Identification of exosomes extracted from plasma

The purification of plasma exosomes was observed by transmission electron microscopy. The purification products of exosomes featured a vesicle-like structure, and the expected size ranged from 50-200 nm, which is consistent with the morphology and size of exosomes (Figure 1A). Nanoparticle tracking analysis (NTA) was used to detect the concentration and diameter of exosomes (Figure 1B). Western blot analysis was performed and revealed that two commonly used exosomal protein markers, namely, HSC70 and TSG101, were highly enriched in the isolated exosomes relative to plasma supernatant (Figure 1C). These results are consistent with previously reported characteristics of exosomes, which confirmed that we had successfully purified exosomes from plasma samples.

3.2 Identification of differentially expressed miRNAs

Twenty-two MI, 12 MIAO and 15 NC peripheral blood serum samples were taken to extract the exosomal miRNA and second-generation sequencing was performed. The measured miRNA was quantified with reads per million (RPM). The distribution of miRNA expression in exosomes varied greatly from person to person (Figure 2A). After bioinformatic analysis, a total of 1,505 miRNAs were annotated, which were considered to be known miRNAs. The distinct expression signatures of healthy individuals and patients with preoperative MI are visualized in the volcano plot in Figure 2B, which shows the upregulation of 514 miRNAs and downregulation of 790 miRNAs. The distinct expression signatures of MI patients after surgery and preoperative patients are visualized in the volcano plot Figure 2C, which shows the upregulation of 47 miRNAs and the downregulation of 94 miRNAs.

3.3 Prediction of target genes of differentially expressed miRNAs before and after intervention therapy of MI and functional enrichment analysis

GO analysis, including biological process (BP), cellular component (CC) and molecular function (MF) analyses, was performed to investigate the function and annotation of the target genes. The 20 terms that were most significantly enriched in these three domains are presented in Figures 3A-C. The differentially expressed genes were closely correlated with the following molecular functions: protein binding, binding, transcription regulator activity, organic cyclic compound binding, heterocyclic compound binding, and enzyme binding. The involved primary biological processes were regulation of cellular metabolic process, cellular macromolecule metabolic process, regulation of primary metabolic process, and organic substance biosynthetic process. The cellular components most strongly associated with the differentially expressed genes were intracellular, intracellular part, intracellular organelle, membrane-bounded organelle, and organelle. Scatter plots were constructed to intuitively illustrate the Kyoto Encyclopedia of Genes and Genomes (KNGG) analysis results. The 20 pathways that exhibited a smaller P value are shown in Figure 3D. The analysis indicated that the signaling pathways with significant correlations included FoxO signaling pathway, Hippo signaling pathway, HIF-1 signaling pathway, Wnt signaling pathway, and mTOR signaling pathway.

3.4 Correlation analysis between strain parameters of RT3D-STE and miRNAs

The correlation between the differentially expressed miRNAs before intervention therapy of MI compared with healthy people and the strain parameters of RT3D-STE were analyzed. An absolute value of Pearson correlation >0.5 and a P value<0.5 were considered as strong correlations. Eighty-one (81) miRNAs had strong correlation with GAS, GLS, GCS and GRS. Among these miRNAs, 5 miRNAs (hsa-miR-4778-3p, hsa-miR-4798-3p, hsa-miR-376c-3p, hsa-miR-371a-3p, and hsa-miR-4735-5p) were found to be differentially expressed before and after intervention therapy of MI (Figure 4A). Three of these miRNAs (hsa-miR-4798-3p, hsa-miR-371a-3p, and hsa-miR-4735-5p) were differentially expressed and inconsistently up- and downregulated between the two groups in MI patients compared with normal samples and after surgical therapy compared with before surgical therapy of MI (Table 1). hsa-miR-4798-3p and hsa-miR-371a-3p were downregulated in MI patients compared with normal samples and upregulated in after surgical therapy compared with before surgical therapy of MI. Besides hsa-miR-4735-5p showed the opposite regulation. These miRNAs were all negatively correlated with GLS. Furthermore, we plotted ROC curves and calculated the area under the curve (AUC). The AUC values of hsa-miR-4798-3p, hsa-miR-371a-3p, and hsa-miR-4735-5p were 0.93, 0.815, and 0.722, respectively (**Supplementary Table 2 and** Figure 4B-D).

3.5 qRT-PCR validation of the differential expression of miRNAs

We employed qRT-PCR to verify the expression levels of hsa-miR-4798-3p, hsa-miR-371a-3p, and hsa-miR-4735-5p. The qRT-PCR results exhibited the same trend of expression changes as the high-throughput sequencing analysis. Specifically, as shown in Figure 5, the expression levels of hsa-miR-4798-3p and hsa-miR-371a-3p were increased, and the expression of hsa-miR-4735-5p was decreased after surgical therapy compared with before surgical therapy of MI.

4. Discussion

MicroRNAs (miRNAs) are single-stranded RNA molecules that measure approximately 21-23 nucleotides in length, and they inhibit protein translation or mRNA degradation by binding to the 3'UTRs of messenger RNAs (mRNAs)[2,29]. Accumulating evidence has demonstrated that miRNAs participate in a variety of biological functions through negative regulatory genes, including cell proliferation, apoptosis, and inflammation, and have a strong correlation with disease mechanisms, especially cardiovascular disease mechanisms. Research shows that miRNAs play important roles in the pathology of myocardial apoptosis, fibrosis, and hypertrophy after MI. Moreover, bulk of of studies have indicated that miRNAs have the potential to serve as alternative biomarkers for the diagnosis of MI. For example, some exosomal miRNAs, such as miR-1, miR-133, miR-208a, and miR-499, are significantly different in MI patients compared with the normal group[21]. Therefore, the identification of miRNAs with different expression levels before and after MI intervention is of great significance for the diagnosis and prognosis of MI.

In this study, we have identified 141 differentially expressed miRNAs after surgical therapy compared with before surgical therapy of MI, including 94 downregulated and 47 upregulated miRNAs. Some of these miRNAs have been reported to be related to MI. Yuan et al. [33] found that miR-144-3p promotes cell proliferation, migration and collagen production by targeting PTEN in myocardial fibroblasts. This indicats that miR-144-3p-mediated PTEN regulation may be a new therapeutic target for myocardial fibrosis after myocardial infarction. Yan et al.[31] found that miR-499a-5p was significantly upregulated in Sudden cardiac death samples compared with control samples, which may serve as an independent diagnostic biomarker for sudden cardiac death. A recent systematic review [28] demonstrated that miR-499a-5p and miR-1-3p are promising MI biomarkers because of their satisfactory diagnostic accuracy and short time window (within 4 hours of symptoms). Velle-Forbord et al.[27] showed that miR-151a-5p can be used as a predictive biomarker of MI. Liu et al. [13] found that miR-199a-5p is upregulated in am ischemia-reperfusion model, and knocking out miR-199a-5p can prevent ischemia-reperfusion-induced cardiomyocyte apoptosis by targeting the HIF-1α-GSK3β-mPTP axis. This indicates that knocking out miR-199a-5p may be a potential target for the treatment of MI patients.

Our research shows that the target genes of these differentially expressed miRNAs after surgical therapy compared with before surgical therapy of MI are significantly correlated with the FoxO signaling pathway, Hippo signaling pathway, HIF-1 signaling pathway, Wnt signaling pathway, and mTOR signaling pathway. Studies[18,25] have shown that these signaling pathways play important roles in cardiac development and diseases. The FoxO fMIly proteins include FoxO1, FoxO3, FoxO4 and FoxO6, Zhu et al.[37] claimed that FoxO4 can promote the early inflammatory response of myocardial infarction through endothelial Arg1. Tian et al.[26] found that the MST1-Hippo pathway is activated in MI and promotes the inflammatory response of cardiomyocytes by inhibiting the HO-1 signaling pathway. The HIF-1 signaling pathway is a stress signaling pathway in hypoxia, that can protect the myocardium by regulating the function of HIF-1α[10,36]. Wnt signaling pathways are essential in heart development and active in the post-MI adult heart[20]. Inhibition of the Wnt signaling pathway has been shown to be beneficial to MI by improving heart remodeling[3]. Studies have shown that mTORC2 has an important anti-remodeling effect on MI[24]. These results suggest that these miRNAs may play important roles in the occurrence and development of MI, and may serve as diagnostic and prognostic markers as well as potential targets for treatment.

STE may be applied to the evaluation of systolic and diastolic dysfunction, and its role in predicting left ventricular remodelling after MI has been confirmed which represents an important prognostic datum[14]. hsa-miR-4798-3p, hsa-miR-371a-3p, and hsa-miR-4735-5p were differentially expressed and inconsistently up- and downregulated between the two groups in AMI patients compared with normal samples and after surgical therapy compared with before surgical therapy for AMI. In addition, they are strongly correlated with GLS. GLS and LVEF are considered to be markers of subclinical LV dysfunction[35]. With the gradual reduction of myocardial perfusion, the LS of the myocardium approximately decrease by 50%. Therefore, it is considered that the reduction in LS may be an important early-stage index to reflect the reduced systolic function of the heart[38]. 3D-GLS can predict long-term prognosis after ST-elevation

acute myocardial infarction (STEMI), and the combination of 3D-GLS and 3D-GCS can improve the accuracy of these predictions[8]. Keeping in mind the above results and discussion, we may claim that these three miRNAs may be used as a prognostic assessment of MI in future.

5. Conclusion

We have identified differentially expressed miRNAs before and after surgical therapy of MI, and their target genes were found to be related with FoxO signaling pathway, Hippo signaling pathway, and Wnt signaling pathway. These miRNAs may play an important role in the occurrence and development of MI. Some of these miRNAs (i.e., hsa-miR-4798-3p, hsa-miR-371a-3p, and hsa-miR-4735-5p) are strongly correlated with GLS and may be used as potential prognostic indicators of MI.

Declarations

Ethics approval and consent to participate

The present study was approved by the Research Ethics Committee of Shenzhen Longhua People's Hospital (NO. KY20200801). The research was conducted with the informed consent of each participant, and all participants have signed the informed consent forms.

Consent for publication

All the authors and patients are agreed to publish.

Competing interests

The authors declare that they have no conflict of interest.

Funding

This work was supported by Shenzhen Science and Technology Innovation Commission Fund No. JCYJ20180228164039703 and MKD202007090221.

Authors' contributions

Xiaozhu Chen: Conceptualization, Methodology, Writing - Original Draft. Fengrong Huang: Methodology, Formal analysis, Writing - Original Draft. Yunhong Liu: Investigation, Visualization. Shujun Liu: Software, Formal analysis.

Acknowledgements

Thanks for every patient participated in this study. It is their disease data that lays the foundation for the subsequent treatment of patients.

Availability of data and materials

The datasets analysed during the current study available from the corresponding author on reasonable request.

References

1. Al Saikhan L, Alobaida M, Bhuva A, Chaturvedi N, Heasman J, Hughes AD, et al. Imaging Protocol, Feasibility, and Reproducibility of Cardiovascular Phenotyping in a Large Tri-Ethnic Population-Based Study of Older People: The Southall and Brent Revisited (SABRE) Study. *Frontiers in cardiovascular medicine*. 2020;7:591946.
2. Cheng M, Yang J, Zhao X, Zhang E, Zeng Q, Yu Y, et al. Circulating myocardial microRNAs from infarcted hearts are carried in exosomes and mobilise bone marrow progenitor cells. Feb 27 2019;10(1):959.
3. Fu WB, Wang WE, Zeng CY. Wnt signaling pathways in myocardial infarction and the therapeutic effects of Wnt pathway inhibitors. *Acta pharmacologica Sinica*. Jan 2019;40(1):9–12.
4. Gong FF, Vaitenas I, Malaisrie SC, Maganti K. Mechanical Complications of Acute Myocardial Infarction: A Review. *JAMA cardiology*. Mar 1 2021;6(3):341–349.
5. Guo M, Li R, Yang L, Zhu Q, Han M, Chen Z, et al. Evaluation of exosomal miRNAs as potential diagnostic biomarkers for acute myocardial infarction using next-generation sequencing. *Annals of translational medicine*. Feb 2021;9(3):219.
6. Henning RJ. Cardiovascular Exosomes and MicroRNAs in Cardiovascular Physiology and Pathophysiology. *Journal of cardiovascular translational research*. Apr 2021;14(2):195–212.
7. Hosseini M, Roshangar L, Raeisi S, Ghahremanzadeh K, Negargar S, Tarmahi V, et al. The Therapeutic Applications of Exosomes in Different Types of Diseases: A Review. *Current molecular medicine*. 2021;21(2):87–95.
8. Iwahashi N, Kirigaya J, Gohbara M, Abe T, Horii M, Hanajima Y, et al. Global Strain Measured by Three-Dimensional Speckle Tracking Echocardiography Is a Useful Predictor for 10-Year Prognosis After a First ST-Elevation Acute Myocardial Infarction. *Circulation Journal*. 2021;advpub.
9. Iwahashi N, Kirigaya J, Gohbara M, Abe T, Horii M, Hanajima Y, et al. Global Strain Measured by Three-Dimensional Speckle Tracking Echocardiography Is a Useful Predictor for 10-Year Prognosis After a First ST-Elevation Acute Myocardial Infarction. *Circulation journal: official journal of the Japanese Circulation Society*. Jun 1 2021.
10. Jain T, Nikolopoulou EA, Xu Q, Qu A. Hypoxia inducible factor as a therapeutic target for atherosclerosis. *Pharmacology & therapeutics*. Mar 2018;183:22-33.

11. Kutty RS, Jones N, Moorjani N. Mechanical Complications of Acute Myocardial Infarction. *Cardiology Clinics*. 2013;31(4):519–531.
12. Lee GK, Hsieh YP, Hsu SW, Lan SJ. *Exploring diagnostic and prognostic predictive values of microRNAs for acute myocardial infarction: A PRISMA-compliant systematic review and meta-analysis.* Medicine (Baltimore). 2021 Jul 23;100(29):e26627. doi: 10.1097/MD.0000000000026627.
13. Liu DW, Zhang YN, Hu HJ, Zhang PQ, Cui W. Downregulation of microRNA–199a–5p attenuates hypoxia/reoxygenation–induced cytotoxicity in cardiomyocytes by targeting the HIF–1α–GSK3β–mPTP axis. *Molecular medicine reports*. Jun 2019;19(6):5335–5344.
14. Lotti R, V DEM, Della Bona R, Porto I, Rosa GM. Speckle-tracking echocardiography: state of art and its applications. *Minerva medica*. May 5 2021.
15. Ludwig N, Leidinger P, Becker K, Backes C, Fehlmann T, Pallasch C, et al. Distribution of miRNA expression across human tissues. *Nucleic acids research*. May 5 2016;44(8):3865–3877.
16. Maguy A, Tardif JC, Busseuil D, Ribi C, Li J. Autoantibody Signature in Cardiac Arrest. *Circulation*. Jun 2 2020;141(22):1764–1774.
17. Mandoli GE, Pastore MC. Speckle tracking stress echocardiography: A valuable diagnostic technique or a burden for everyday practice? Dec 2020;37(12):2123–2129.
18. Mia MM, Singh MK. The Hippo Signaling Pathway in Cardiac Development and Diseases. *Frontiers in cell and developmental biology*. 2019;7:211.
19. Ojha R, Nandani R, Pandey RK, Mishra A. Emerging role of circulating microRNA in the diagnosis of human infectious diseases. Feb 2019;234(2):1030–1043.
20. Ozhan G, Weidinger G. Wnt/β-catenin signaling in heart regeneration. *Cell regeneration (London, England)*. 2015;4(1):3.
21. Pinchi E, Frati P. miR-1, miR-499 and miR-208 are sensitive markers to diagnose sudden death due to early acute myocardial infarction. Sep 2019;23(9):6005–6016.
22. Reed GW, Rossi JE, Cannon CP. Acute myocardial infarction. *Lancet (London, England)*. Jan 14 2017;389(10065):197–210.
23. Reyes-Retana JA, Duque-Ossa LC. Acute Myocardial Infarction Biosensor: A Review From Bottom Up. *Current problems in cardiology*. Mar 2021;46(3):100739.
24. Sciarretta S, Forte M, Frati G, Sadoshima J. New Insights Into the Role of mTOR Signaling in the Cardiovascular System. *Circulation research*. Feb 2 2018;122(3):489–505.
25. Shimizu H, Langenbacher AD. The Calcineurin-FoxO-MuRF1 signaling pathway regulates myofibril integrity in cardiomyocytes. Aug 19 2017;6.
26. Tian Y, Song H, Jin D, Hu N, Sun L. MST1-Hippo pathway regulates inflammation response following myocardial infarction through inhibiting HO-1 signaling pathway. *Journal of receptor and signal transduction research*. Jun 2020;40(3):231–236.
27. Velle-Forbord T, Eidlaug M, Debik J, Sæther JC, Follestad T, Nauman J, et al. Circulating microRNAs as predictive biomarkers of myocardial infarction: Evidence from the HUNT study. *Atherosclerosis*.

Oct 2019;289:1–7.

28. Wang B, Li Y, Hao X, Yang J, Han X, Li H, et al. Comparison of the Clinical Value of miRNAs and Conventional Biomarkers in AMI: A Systematic Review. *Frontiers in genetics*. 2021;12:668324.
29. Wang Q, Liu B, Wang Y, Bai B, Yu T, Chu XM. The biomarkers of key miRNAs and target genes associated with acute myocardial infarction. *PeerJ*. 2020;8:e9129.
30. Wexler Y, Nussinovitch U. The Diagnostic Value of Mir-133a in ST Elevation and Non-ST Elevation Myocardial Infarction: A Meta-Analysis. *Cells*. 2020;9(4):793.
31. Yan F, Chen Y, Ye X, Zhang F, Wang S, Zhang L, et al. miR-3113-5p, miR-223-3p, miR-133a-3p, and miR-499a-5p are sensitive biomarkers to diagnose sudden cardiac death. *Diagnostic pathology*. Jul 31 2021;16(1):67.
32. Yeh RW, Sidney S, Chandra M, Sorel M, Selby JV, Go AS. Population trends in the incidence and outcomes of acute myocardial infarction. *The New England journal of medicine*. Jun 10 2010;362(23):2155–2165.
33. Yuan X, Pan J, Wen L, Gong B, Li J, Gao H, et al. MiR-144-3p Enhances Cardiac Fibrosis After Myocardial Infarction by Targeting PTEN. *Frontiers in cell and developmental biology*. 2019;7:249.
34. Yuda S. Current clinical applications of speckle tracking echocardiography for assessment of left atrial function. *Journal of Echocardiography*. 2021/09/01 2021;19(3):129-140.
35. Zamorano JL, Lancellotti P, Muñoz DR, Aboyans V, Asteggiano R, Galderisi M, et al. [2016 ESC Position Paper on cancer treatments and cardiovascular toxicity developed under the auspices of the ESC Committee for Practice Guidelines]. *Kardiologia polska*. 2016;74(11):1193–1233.
36. Zhang Z, Yao L, Yang J, Wang Z, Du G. PI3K/Akt and HIF–1 signaling pathway in hypoxia–ischemia (Review). *Molecular medicine reports*. Oct 2018;18(4):3547–3554.
37. Zhu M, Goetsch SC, Wang Z, Luo R, Hill JA, Schneider J, et al. FoxO4 promotes early inflammatory response upon myocardial infarction via endothelial Arg1. *Circulation research*. Nov 6 2015;117(11):967–977.
38. Zhu W, Liu W, Tong Y, Xiao J. Three-dimensional speckle tracking echocardiography for the evaluation of the infarct size and segmental transmural involvement in patients with acute myocardial infarction. *Echocardiography (Mount Kisco, N.Y.)*. 2014;31(1):58–66.

Figures

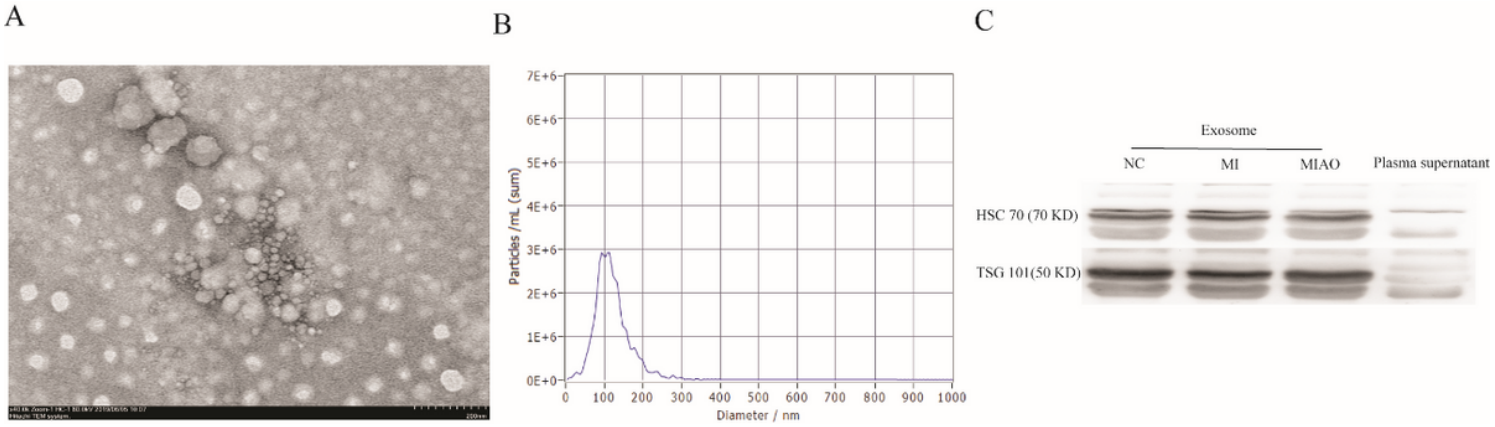

Figure 1

Characterization of exosomes. **(A)** Isolated exosomes micrograph of transmission electron microscopy. **(B)** Concentration and diameter of isolated exosomes as detected by nanoparticle tracking analysis (NTA). (C) Exosome protein markers validation by western blotting.

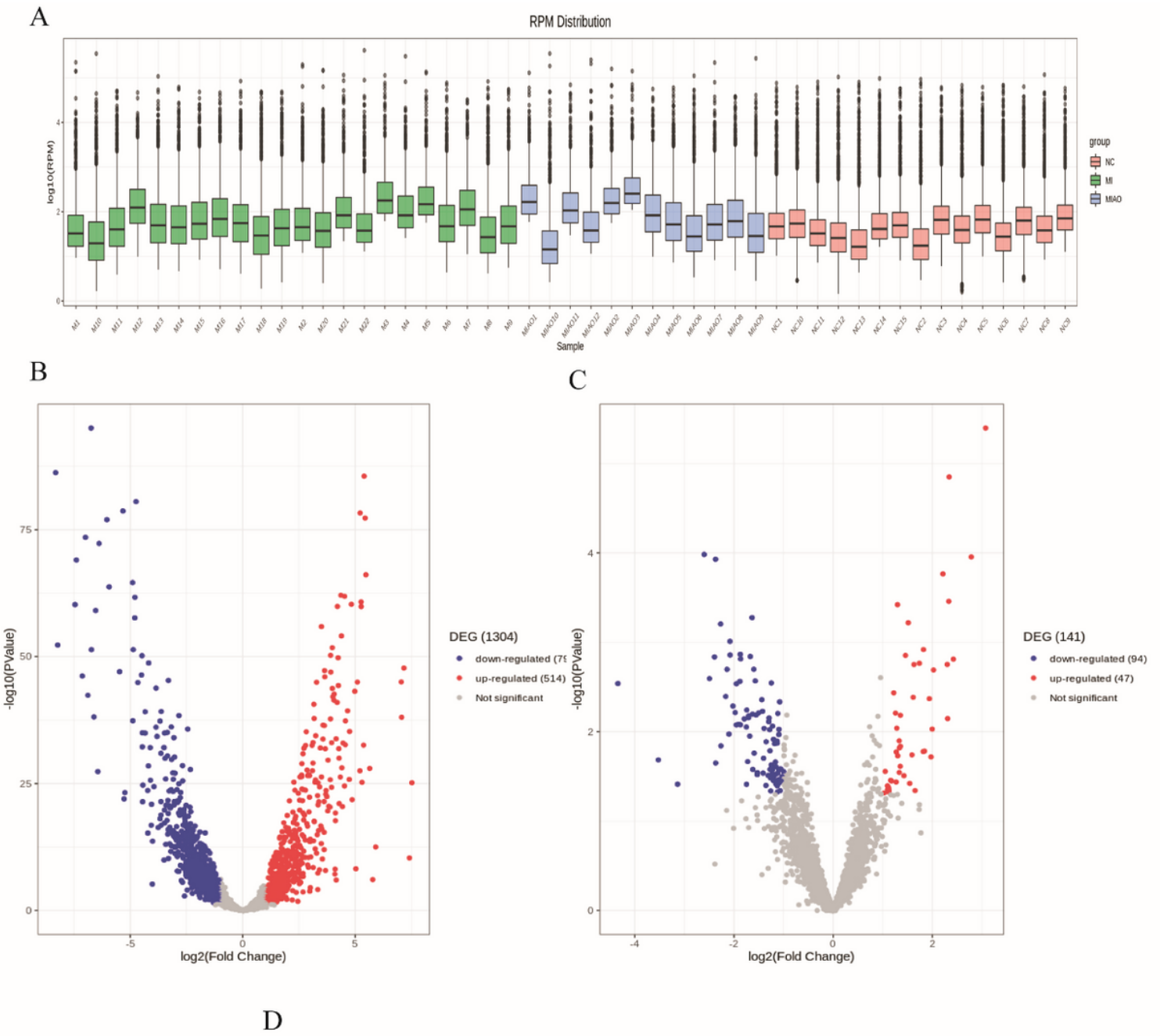

Figure 2

Identification of differentially expressed miRNAs. (A) miRNA abundance distribution of exosomes in each sample, calculated as read per million (RPM). **(B)** Volcano based on the differential expression of the altered miRNAs in the patients with preoperative MI group and healthy individual group. Columns represent serum samples, and rows represent miRNAs. Red indicates high expression, and blue indicates low expression. **(C)** Volcano based on the differential expression of the altered miRNAs in patients with MI before and after surgery.

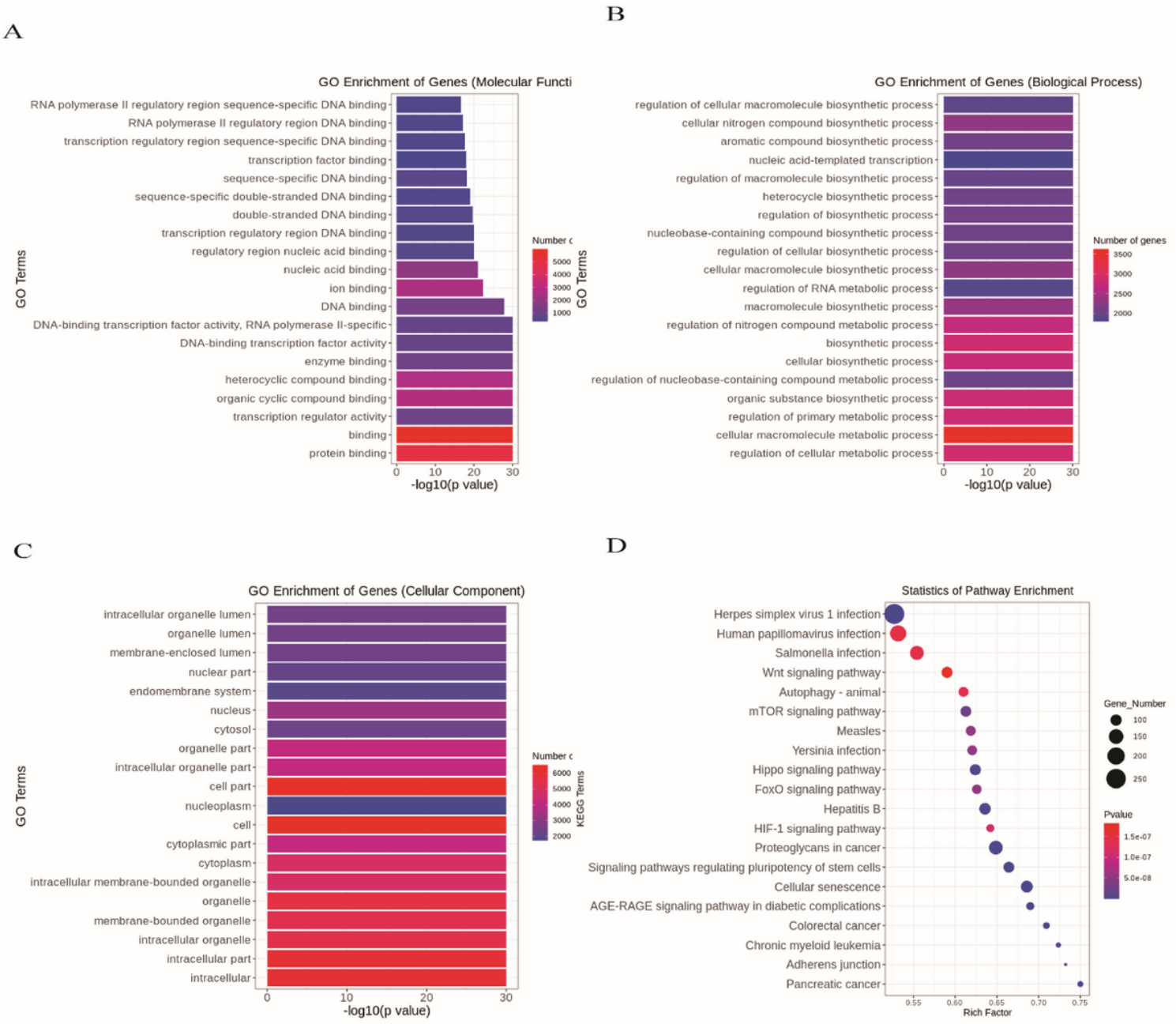

Figure 3

Top 20 functional GO terms and KEGG pathways of the differentially expressed miRNA target genes shown according to p-value. (A) Molecular Function terms, (B) Biological Process terms, (C) Cellular Component terms, (D) Top 20 KEGG pathways.

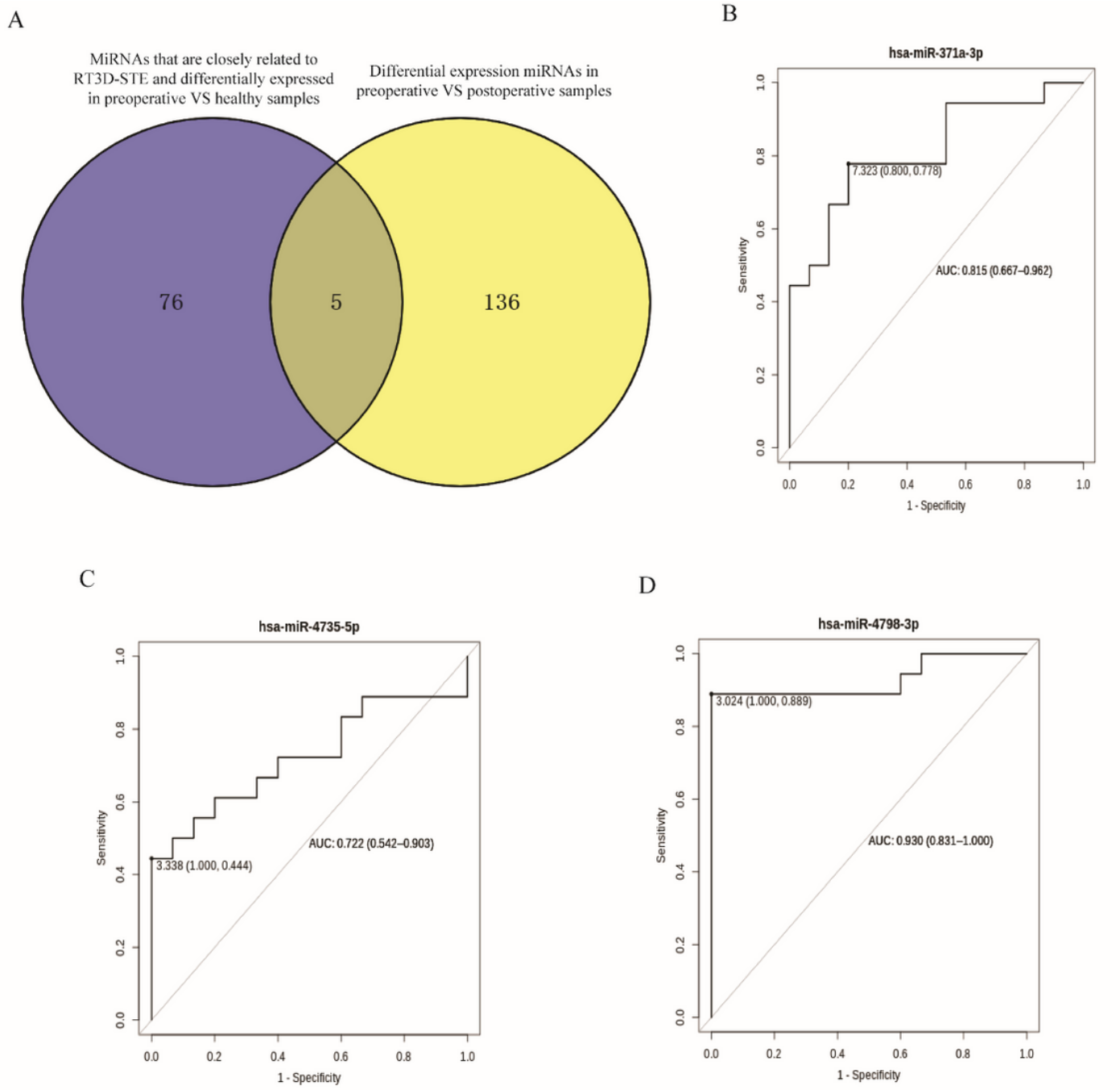

Figure 4

(A)Venn diagrams of differential expression miRNAs strongly correlated with RT3D-STE in preoperative VS healthy samples and differential expression miRNAs in preoperative VS postoperative samples. ROC curves of (B) has-miR-371a-3p, (C) has-miR-4735-5p, and (D)has-miR-4798-3p.

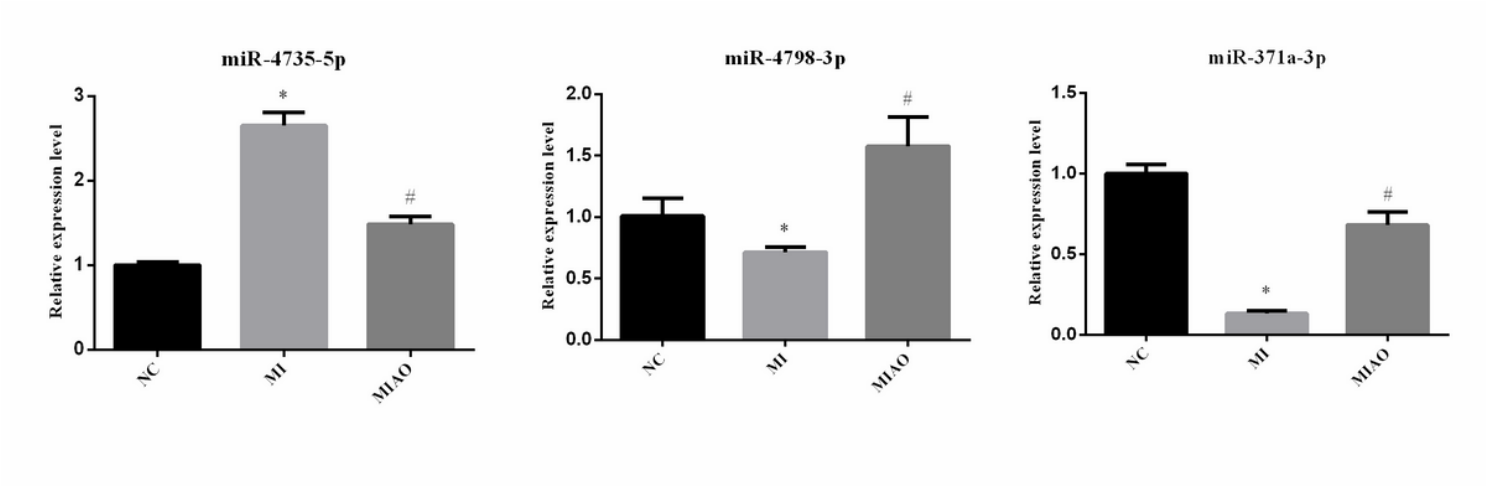

Figure 5

Sequencing results were verified by qRT-PCR. Relative Expression level of (A) hsa-miR-4798-3p, (B) hsa-miR-371a-3p, and (C) hsa-miR-4735-5p in preoperative compared with postoperative of MI (n = 3 biological replicates for each assay, mean ± SEM, * compared with Normal $p<0.05$, # compared with NSTEMI $p<0.05$ one-way AVOVA)

Supplementary Files

This is a list of supplementary files associated with this preprint. Click to download.

- SupplementaryTable1.docx
- SupplementaryTable2.docx
- originalfigureofWB.zip